Bulletin of the Earthquake
Research Institute
Vol. 54 (1979), pp. 441-462

19. *Mechanism of the Earthquake Swarm Activity in the Kawanazaki-oki, Izu Peninsula, as Inferred from the Analysis of Seismic Waveforms.*

By Masaru Tsujiura,
Earthquake Research Institute.

(Received September 14, 1979)

Abstract

The earthquake swarm activity which occurred in the Kawanazaki-oki area of the Izu peninsula is studied through the analysis of waveforms. The earthquakes are usually concentrated within a brief time interval (e.g., 1 hour); they usually share a similar waveform; and the arrival times for certain isolated waves, measured from the *P*-wave onset of their events, are the same within a deviation of 0.05 sec (0.02 sec for the events with similar size). Similar behavior, but with different waveforms, can be seen for the earthquakes which occurred in another time interval. Nineteen event groups, with their own spectral characteristics, are obtained for 264 earthquakes selected from 365 earthquakes. In addition, the corner frequency of the source spectrum in a given event group is constant, that is independent of earthquake magnitudes between 1.5 and 3. From the points of waveform and spectrum, we suggest that there exist numerous cracks and faults bounded by strong barriers, and the earthquakes in a given event group are occurring over the same fault as repeated stick-slip.

Introduction

Many studies have been made on the space-time distribution of earthquake occurrence. Besides those studies, we make special reference to the paper of Mogi (1963) which relates that phenomenon to the medium structure. Mogi distinguished three types of earthquake patterns according to material characteristics and pointed out that activity in an extremely heterogeneous medium reveals swarm type earthquakes. Kasahara and Teisseyre (1966) discussed the development of swarm activity on the basis of a dislocation theory.

Recently, earthquake prediction is becoming a social demand. When seismic activity is increasing in a certain region it is very important to discriminate the foreshocks preceding a large earthquake from the swarm activity without major earthquakes. In some cases special

spectral features of foreshocks were found for certain regions (TSUJIURA, 1977, 1978b).

Since Nov. 24, 1978, a swarm activity started in the Kawanazaki-oki, Ito area of the Izu peninsula and its activity continued for about 20 days (TSUMURA *et al.*, 1979). A similar swarm activity in this area occurred in 1930 (e.g., KISHINOUYE, 1937). In this paper, we study spectral features of seismic waves from the swarm. We shall show some interesting features of the waveform and relate it to the mechanism of swarm activity. If such features are commonly observed for other swarms, present results may be used for the discrimination of swarm activity from other earthquake activity such as foreshocks (TSUJIURA, 1979).

Data

In order to determine the spectral contents of the seismic waves, analog-type spectral analyzers have been operated on a routine basis. A detailed description of the analyzer system was given by TSUJIURA

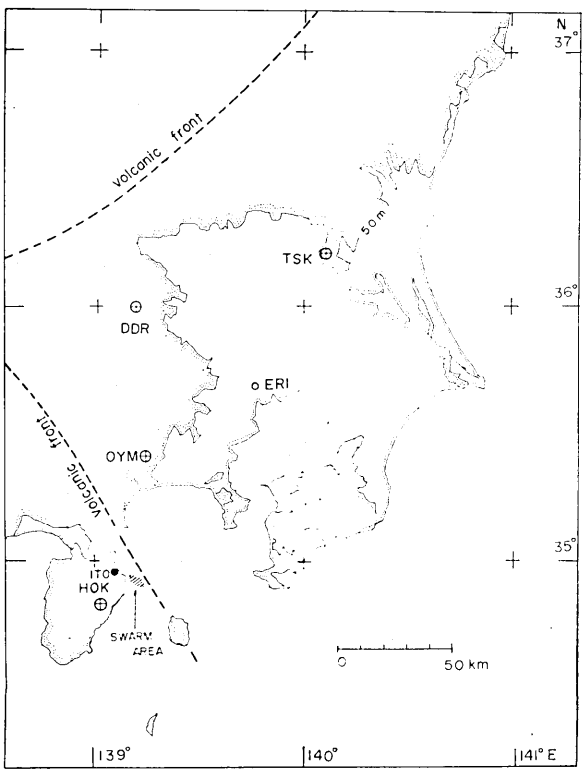

Fig. 1. The seismic telemetering stations used in the present study.

(1966, 1978a). A brief outline of the system will be described in the following.

The analyzer consists of one amplifier, six band-pass filters with center frequencies at 0.75, 1.5, 3, 6, 12 and 24 Hz, and respective bandwidths of 0.5, 1, 2, 4, 8 and 16 Hz. The output of the six filters is recorded continuously on an ink-writing 6-channel recorder. The input of the amplifier is connected to the output of the seismic telemetering network in the Kanto district. Three sets of the identical analyzer are continuously operating for routine observation.

In the course of examining records of the analyzer, we noticed that the earthquake swarm consists of events having similar spectra. In order to examine the waveforms of such earthquakes, a similar analyzer at a high paper speed with a trigger system has been operated since Nov. 29. In this analyzer, an original signal is added instead of the signal of 0.75 Hz band. Figure 1 shows the location of the seismological station.

Two different sets of the data are available for the present analysis. One is the data from three sets of identical analyzers (BPF-1) connected to the E-W component at OYM, DDR and TSK, and the other is the

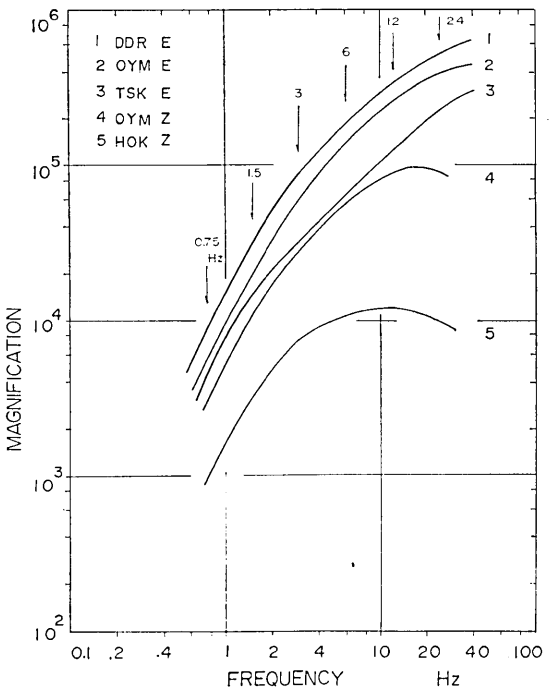

Fig. 2. Magnification curves of the seismograph including seismometer, preamplifier and band-pass filter. Arrows show the center frequencies of the band-pass filters.

data obtained by the same type analyzer connected to the vertical component (Z) at OYM (BPF-2). Figure 2 shows the displacement magnification curves of the analyzer including the response of the seismometer, preamplifier and filter. Arrows show the center frequency (f_0) for each band-pass filter. The magnification of the seismographs for the three stations is nearly the same. Because of the high magnification of the seismograph and the location of the station, the combined data from three stations covers a wider dynamic range. In addition, DDR has a magnetic tape recording system consisting of various kinds of seismographs, such as medium-period, long-period and wide-band (TSUJIURA, 1973). These data are also available for the analysis of larger earthquakes.

Figure 3 shows the seismogram of an event with magnitude (M) of 2.4 obtained by the BPF-2. The paper speed is adjusted to be 25 mm/sec to see the detailed waveforms. The upper trace is the original unfiltered seismogram and the lower five seismograms show the filtered ones. The center frequency of each band-pass filter is shown on the left.

Figure 4 shows an example of the filtered records obtained by the

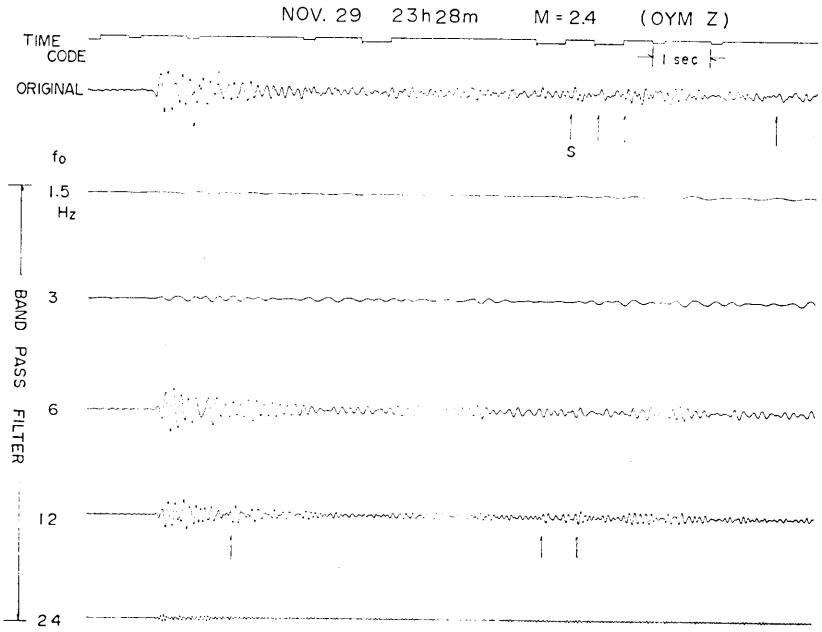

Fig. 3. An example of the seismogram of earthquake with magnitude (M) 2.4 obtained by the trigger system. The upper seismogram shows the original one and the lower five seismograms show the filtered ones. The center frequencies of the band-pass filters (f_0) are shown on the left hand side. Tick marks at the top are second marks superposed on the time code.

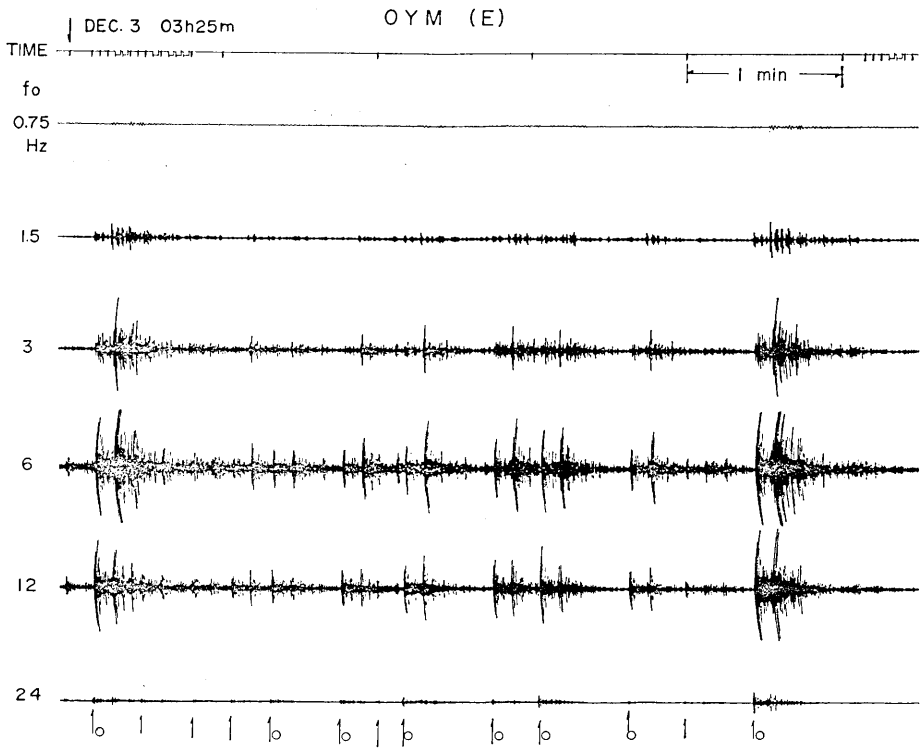

Fig. 4. An example of the filtered seismogram in the most active stage of the swarm obtained at the OYM station ($\Delta \approx 55$ km). Arrows show the *P*-wave onset recognized from the spectrum. The center frequencies of the band-pass filters are shown on the left hand side. Tick marks at the top are minute marks with time code at every 5 minutes.

BPF-1 connected to OYM-E for the events in the most active stage of the swarm. Arrows show the *P*-wave onset of each event recognized from the spectrum, and arrows with an open circle show the events exceeding a threshold of the trigger level. The smallest event in the triggered seismograms corresponds to a magnitude of about 1.5. The magnitude is determined initially by using the formula of HORI (1973) based on the total duration time of seismic waves. As seen in this figure, the earthquakes are generating continuously, therefore the total duration time of seismic oscillation for most events cannot be obtained because of the contamination by the coda waves of former events. In such cases their magnitudes are determined from the relative amplitudes compared with the events with known magnitudes. The seismograms of 365 events with $M > 1.5$ are then obtained by the BPF-2 through the swarm sequence of Nov. 29-Dec. 10. Although our data is missing for smaller events, general properties of the swarm activity on the

basis of waveforms will be obtained. We shall start with the comparison of waveforms.

Analysis of waveforms

In the course of examining the records obtained by the BPF-2, it

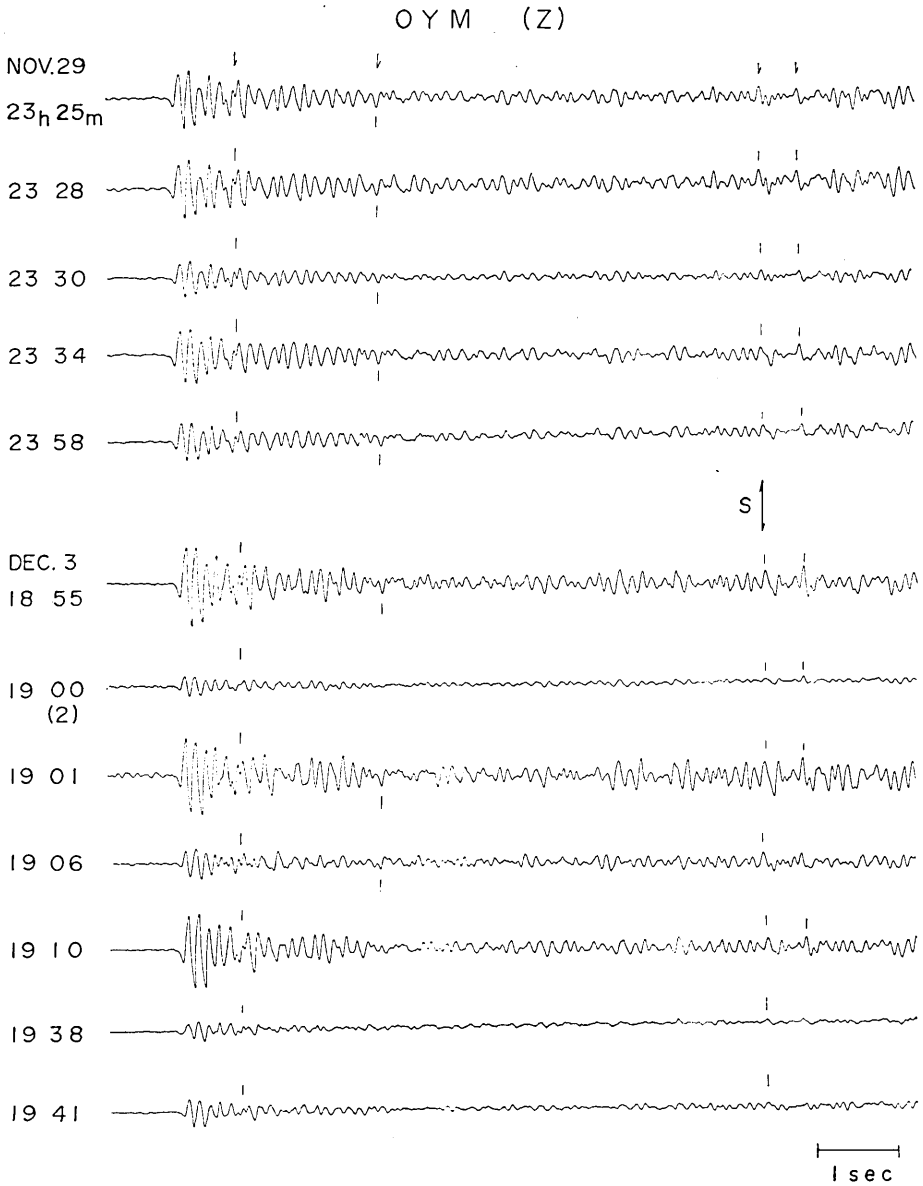

Fig. 5. An arrangement of the seismograms with similar waveforms obtained by the trigger system at OYM. Note the high correlation of the corresponding traces between the seismograms.

was found that there exists a group of earthquakes with similar waveforms. For example, Figure 5 shows an arrangement of the seismograms for some events with similar waveforms. High correlation between the corresponding traces including *P*, *S* and several other isolated phases are clearly seen, especially when the events with similar size are compared. The principal criterion for the selection is made by a visual correlation, superimposing the seismograms on each other. It is an easy procedure, because most of the seismograms of earthquake swarms, in a limited time interval (e.g., 1 hour), belong to one or two patterns with distinct spectral signatures. The seismograms of excluded events in this procedure are again examined through the earthquake sequence. In this procedure, when the earthquakes having a similar waveform numbered more than five we registered them as one group

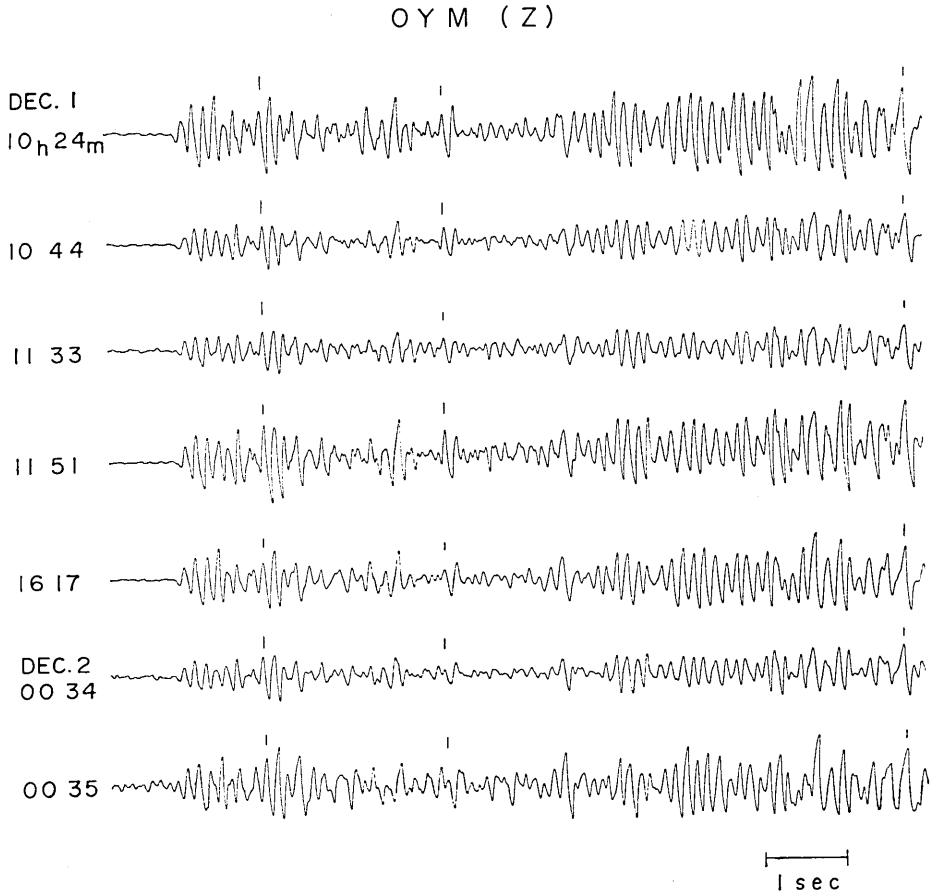

Fig. 6. An arrangement of the seismograms with similar waveforms, but different from those presented in Fig. 5. The arrival times for isolated waves measured from the *P*-wave onset are constant within a range of 0.05 sec.

of similar earthquake or an earthquake family. Although our criterion for the selection is somewhat uncertain the seismograms will give us more reliable answers.

Figure 6 shows the same type of comparison among waveforms of another event group. The peaks and troughs for each corresponding waves again appear to agree well with each other, and such similarity often extends through the coda waves, that is, beyond the *S* and surface waves arrival. The comparison of waveforms is also achieved by the filtered seismograms (see Fig. 3). We found that the peaks and troughs of the wave traces coincided well even in the high frequency components of the 12 Hz band. Figure 7 shows another event group. The reappearance of similar waveforms is confirmed for many earthquakes generated at an interval of 1 to 3 minutes.

Another important feature of similar earthquakes is that the similarity is apparently independent of the earthquake size. Figure 8

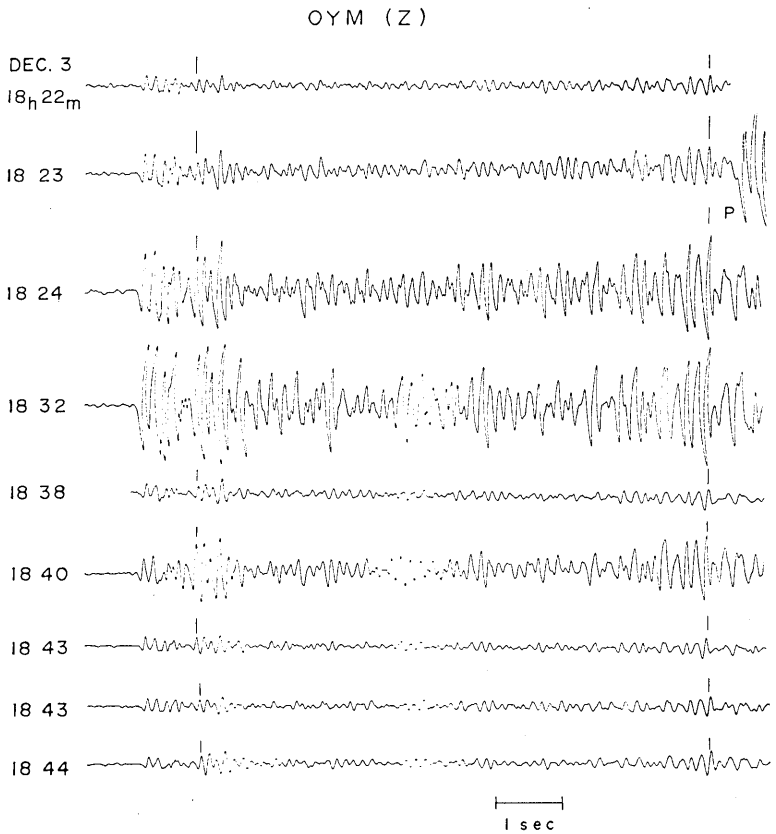

Fig. 7. An arrangement of the seismograms with similar waveforms. An appearance of similar waveforms is confirmed for many earthquakes generated at a short time interval.

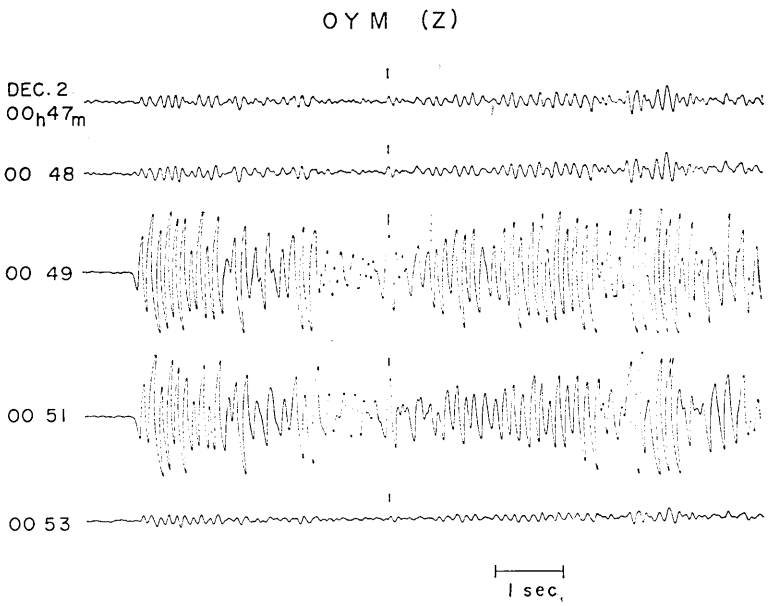

Fig. 8. An arrangement of the seismograms with similar waveforms. Note a similarity of waveforms is independent of earthquake size.

shows the same example of similar earthquakes. Even if the sizes of these events differ by more than a factor of 1 in magnitude unit, the similarity of the P phase and several other phases indicated by arrows is clearly demonstrated. These facts suggest that the spectra of the events with similar waveforms do not depend on the earthquake magnitude. This effect will be discussed further in the section on spectral analysis.

As seen in the previous four figures, there exist event groups with similar waveforms, each of which has a unique waveform character. Figure 9 shows the number of earthquakes recorded every four hours for a 12 day period. The open part of the rectangle shows the number of events belong to some earthquake groups, each of which contains at least five earthquakes with a similar waveform, and the shaded part shows a number of events which do not. The closed part shows those of the clipped events due to the scale out of the recording galvanometer during which no examination of the waveform was possible for classification. Magnitudes determined at our station for those clipped events are indicated in each corresponding place. These magnitudes agree with those determined at JMA within a range of 0.2 unit. The main event in this period is the earthquake with $M=5.5$.

The 264 events having similar waveforms out of 365 events, including the 12 clipped events, were found by visual examination. As is

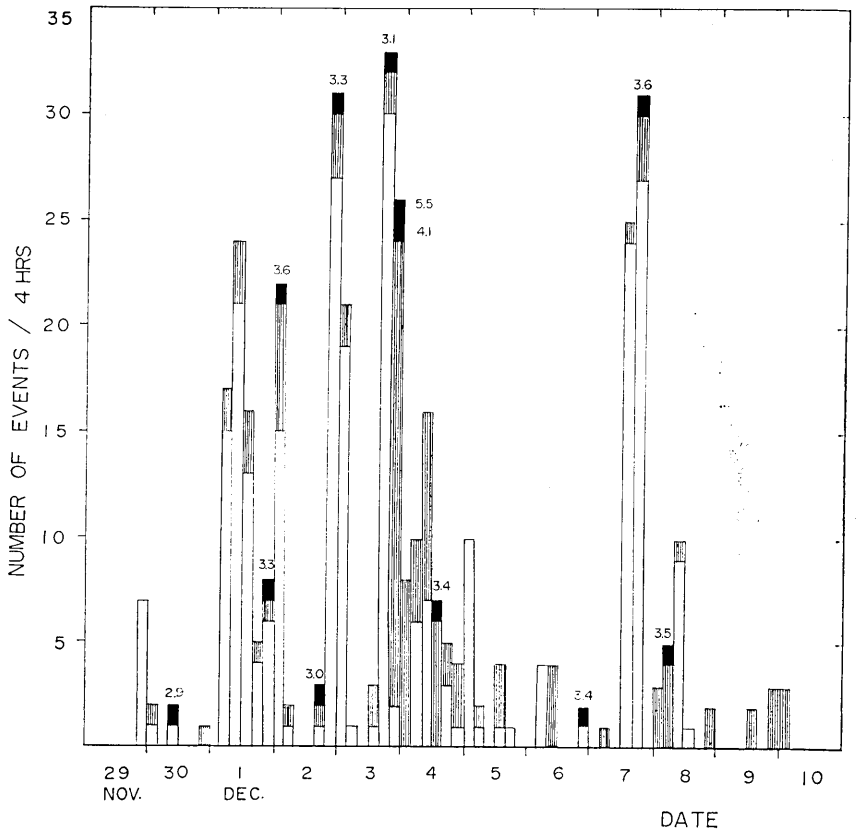

Fig. 9. Number of earthquakes during every 4 hours for a 12 day period obtained at OYM. The open rectangle shows a number of earthquakes belonging to event groups with similar waveforms. Each group consists of more than 5 earthquakes. The shaded part shows a number of events with isolated waveforms. The closed part shows those of the clipped events. Numerals attached to closed parts show a value of magnitude determined at DDR.

seen in this figure, the similar earthquakes are distributed at a high rate of 72% over a whole activity. However, close scrutiny of this figure shows that the rate of occurrence of similar earthquakes decreases after the date of Dec. 3 when the largest event, with $M=5.5$, occurred. The source mechanism of the $M5.5$ event, as well as some other events, is somewhat different when compared with that of the remaing events. We studied the polarity of the initial motion for the 365 events on the basis of the data of OYM. All data showed compressional first motions except for the 8 events that occurred after the $M5.5$ event and a foreshock with $M=4.1$. Therefore, at least the 10 events with different initial motion may be related directly to the $M5.5$ event, forming a sequence of foreshock, main shock and aftershock. The difference in

the rate of occurrence of similar earthquakes will be in part due to the difference of nature between the aftershock and the swarm activity. The epicenter of the $M5.5$ event also does not agree with the area of main swarm activity (see TSUMURA, *et al.*, 1979). Thus, we may separate the $M5.5$ event and its' fore and aftershocks from the present study of swarm activity.

The earthquake swarm consists mainly of a large number of event groups, in which each group has its own spectral signature. For a better explanation, a tentative number is attached to each group. Figure 10 shows the distribution of the event group. A more detailed description of the separation of event groups will be given by the Table in a later section, together with the results of the spectral analysis. We found that the swarm activity during the 12 day period consisted mainly of 19 event groups, where each group has at least five similar earthquakes. The separation of the groups within brackets is somewhat uncertain because the corner frequency of the source spectrum is slightly different between them, although the waveforms are apparently the same (see Table 1). This figure also shows that the swarm activity in a limited time interval (e.g., 1 hour) consists of a small number of event groups, and most activities of these groups

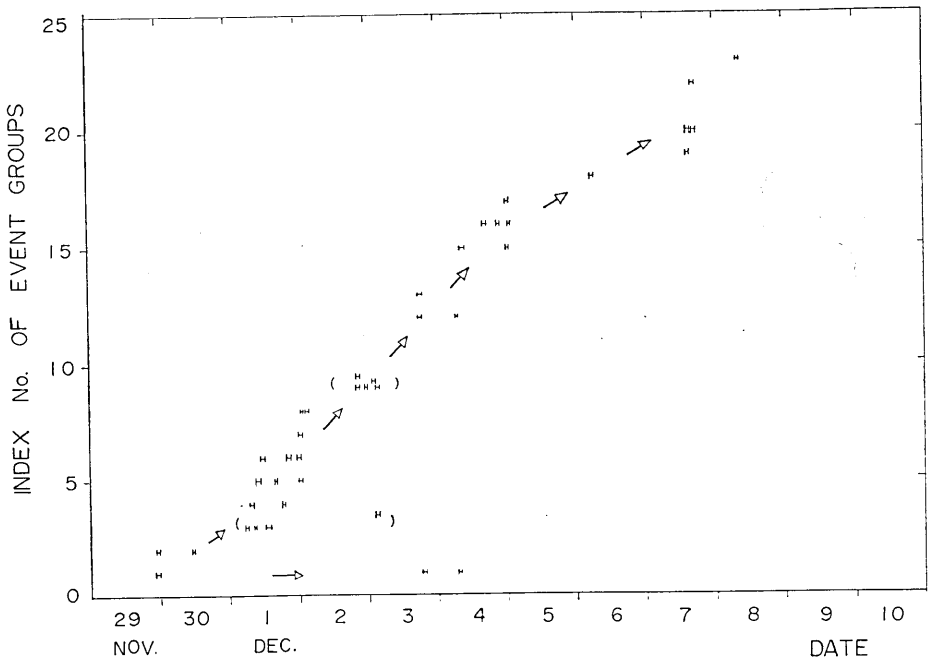

Fig. 10. Distribution of earthquake groups where each group has its own spectral signature. The separation within brackets is somewhat uncertain owing to a different source spectrum.

are finished within one day, except the No. 1 event group where the activity is repeated after about 4 days. If we assume that the epicenters of similar earthquakes are distributed only in a narrow area this figure suggests the migration of swarm activity.

Epicentral location

The earthquakes with similar waveforms have been observed in other seismic regions although the rate of occurrence is low compared with the present earthquake swarm (STAUDER and RYALL, 1967; TSUJIURA, 1973; HAMAGUCHI and HASEGAWA, 1975 and TSUJIURA, 1977). Hamaguchi and Hasegawa suggested that similar earthquakes are closely distributed in space within a range of 5 km. Recently, one event pair with similar waveforms was found in a sequence of the Izu-Oshima-kinkai earthquake of 1978 (TSUJIURA, 1978b). The epicenter of this event pair, determined at JMA, indicates that they are closely located within a range of error of the determination. The epicenters of the events with similar waveforms obtained here are examined by the use of travel time data from the temporary stations distributed in the Izu peninsula (TSUMURA, *et al.*, 1979).

As is seen in the previous figures, the earthquake swarm consists of many earthquakes occurring continuously. Such continual occurrence

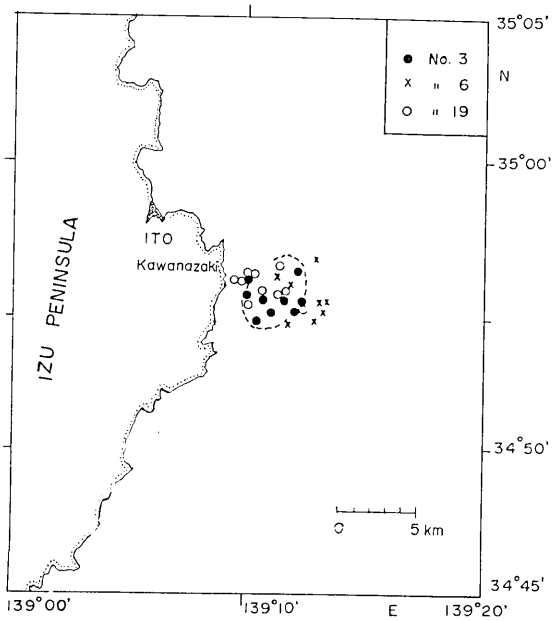

Fig. 11. Epicentral distribution of earthquakes belonging to the three event groups.

will affect the accuracy of the determination of epicenters. Figure 11 shows the epicenters of events commonly obtained for the three event groups. The dotted circle shows the range of epicenters of the No. 3 event group. The location of the events is distributed in space over a range of about 3 km. Considering the exact agreement of waveforms, the epicentral area of 3 km for one event group seems to be too large. As shown in the previous four figures, the similarity of waveforms is very striking within each event group. Moreover, we noted that the arrival times of S and other isolated waves measured from the P-wave onset are constant within a fluctuation of 0.05 sec, and most events

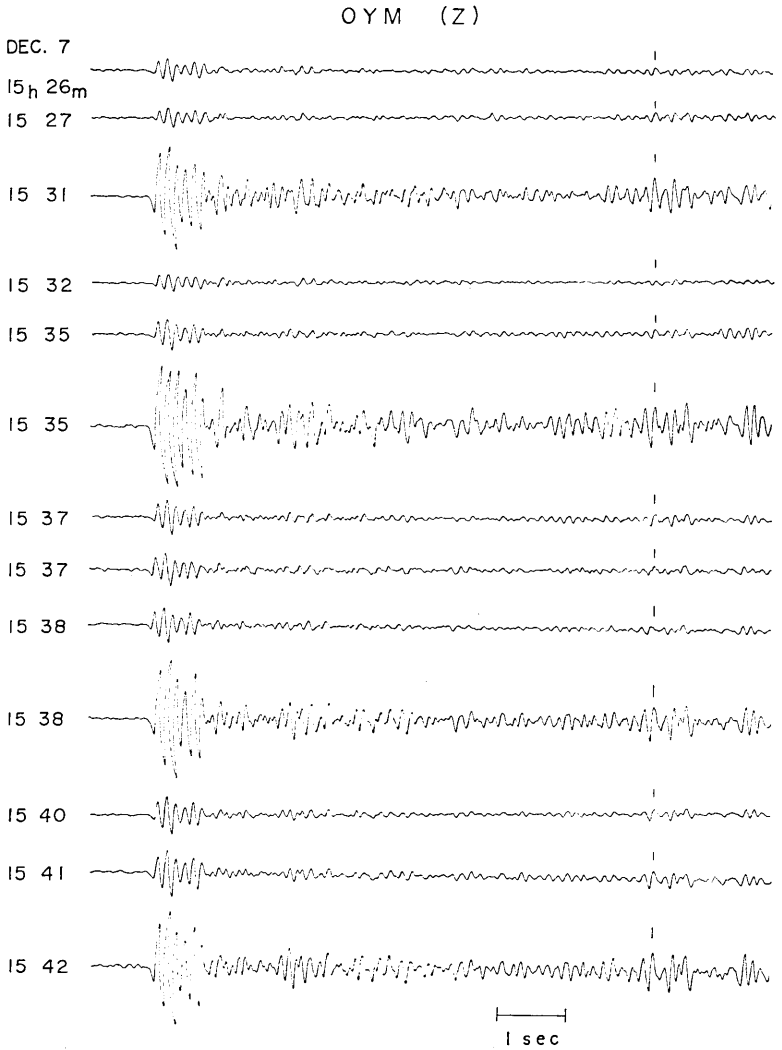

Fig. 12a. Comparison of waveforms for the earthquake family observed at OMY.

with similar size fall to within a range of 0.02 sec which is the accuracy limit of our determination of time. Similar agreements are seen even in the coda waves with a lapse time of 20 sec after the *P*-wave arrival. The similar time differences for body and coda waves suggest that the location between the events with similar waveforms may not differ by as much as the spread of locations determined by Tsumura. For a rough estimation, if we assume that the velocity of our coda waves is 2 km/sec, a time difference of 0.05 sec corresponds to a space difference of 100 meters. Thus, we may suggest that the epicenters of similar earthquakes are the same in a spatial range of 100 meters.

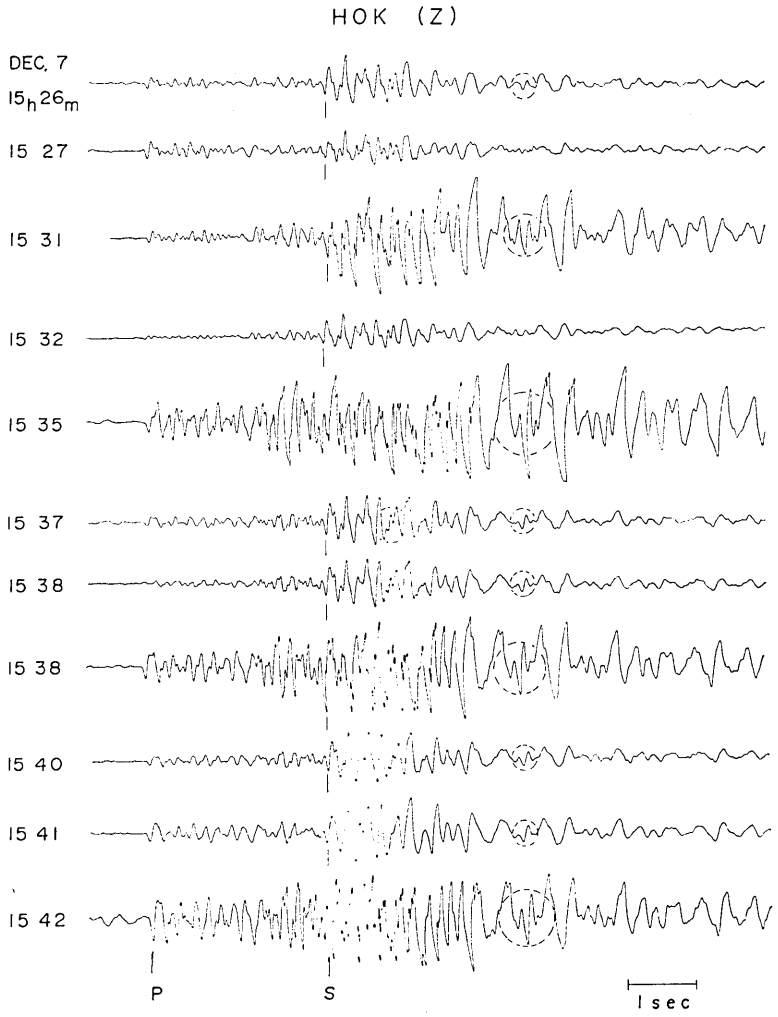

Fig. 12b. Comparison of waveforms observed at HOK for the same earthquakes presented in Fig. 12a.

For further examination of the observations described above, a comparison of waveforms for the same events obtained at two stations located in different directions from the swarm area will be useful. The data of the Hokiyama station (HOK) are selected from our station arrangement (Fig. 1), and the observation at HOK was carried out from Dec. 7, by the same system as at OYM and with a low magnification (Fig. 2).

Figure 12a and-b show the seismograms for the same events obtained by each Z component at OYM and HOK. A clear similarity of waveforms is seen among the seismograms at OYM (a), and the arrival times of S and later phases measured from P-wave onset also agree within the 0.05 sec range, as those presented in previous figures. Similar results are seen in the seismograms of HOK (b). The data of shorter epicentral distance ($\Delta \approx 10$ km) shows more detailed similarity in the frequency range up to 10 Hz. Isolated wavelets, as indicated by dotted circles, are commonly observed even in the coda waves. The agreement of waveforms and arrival times in the two stations suggests more strongly that the seismic waves of their events are comming from the same place within an area of the linear dimension of 100 meters.

As is seen in previous figure No. 10, the activity in a given time interval consists of one or two similar earthquake groups. The existence of the 19 event groups then will be a fact reflecting the migration of swarm activity. Detailed study of the migration compared with the epicentral location will be useful for better understanding the mechanism of swarm activity. According to Tsumura's result, the earthquake swarm is concentrated to an area of 5×8 km. The separation of 19 event groups by Tsumura's data seems to be difficult if we consider the error of determination and the total swarm area. The lack of accuracy in epicentral location, unfortunately, prevents a difinite answer to this problem.

Spectral analysis

In order to obtain the source parameter of similar earthquakes the spectral analysis is made for S waves using the data of BPF-1 described in the previous section. The method of analysis is the same as those of our previous studies (TSUJIURA, 1977, 1978b). The maximum amplitudes (peak to peak) for S waves are measured directly on 6 band filtered traces. Following AKI and CHOUET (1975), the spectral density from the records of band-pass filters is given as

$$f_m = 2(2F\Delta f)$$

where F is a spectral density and Δf is a bandwidth for a given channel.

From the known bandwidth of the band-pass filter and the maximum amplitude of the S waves measured on each frequency, the amplitude spectral density $F(\omega)$ is estimated.

In order to correct the effects of attenuation, spectral amplitudes $F(\omega)$ are multiplied by an exponential term $\exp(-\pi f t/Q_\beta)$, where t is the travel time of the S wave, f is the frequency and Q_β is the quality factor.

The source spectra of S waves for the 264 events belonging to earthquake families are obtained by the method described above. Figure 13 shows the source spectrum for four selected event groups obtained by assuming a value of Q_β 300 (TSUJIURA, 1978b), a shear-wave velocity of 3.5 km/sec and by the site correction dividing the observed spectrum by 2 for $f \leq 1.5$ Hz (TSUJIURA, 1978a). The identification numbers are the same for those presented in Fig. 10. The amplitude of the 0.75 Hz band is not considered in determining the spectrum, because its amplitude is too small to analyze such small earthquakes. The amplitude

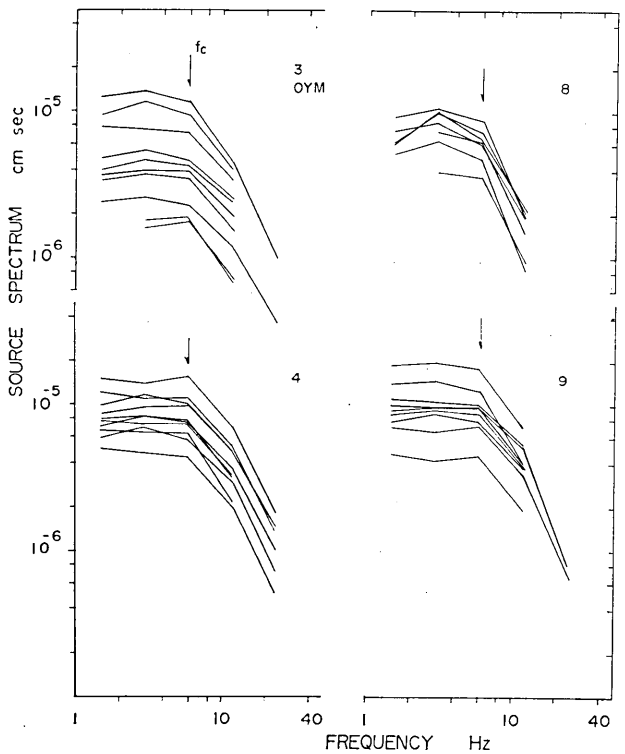

Fig. 13. An example of the source spectra of *SH* waves observed at OYM corrected for attenuation using the values of $Q_\beta=300$, $\beta=3.5$ km/sec and the site factor. Arrows show the corner frequency (f_c). Numerals attached to each spectrum show the index number of the earthquake families.

of 24 Hz band is also excluded for some events because of the poor signal to noise ratio.

The long-period spectral level (Ω_0) and corner frequency (f_c) are determined by fitting the spectra in two straight lines that intersect at the corner frequency. The approximate corner frequency is indicated by arrows. It is noted that the corner frequency in a given event group shows the same value within an error of 30%, independent of the absolute value of amplitudes, except that there are minor differences in the shape of high frequency components. Figure 14 shows the source spectrum for the other event groups. Although the corner frequencies of two event groups in No. 15 and in No. 20 are slightly lower than the former groups, again the corner frequencies agree very well within the group.

In order to obtain the spectrum for a wide dynamic range the data from the other two stations equipped with the same system may be used. The source spectrum obtained at two stations OYM and DDR are shown for the No. 12 event group in the same figure. In obtaining the source spectrum at DDR, a value of Q_β 500 is assumed as a correc-

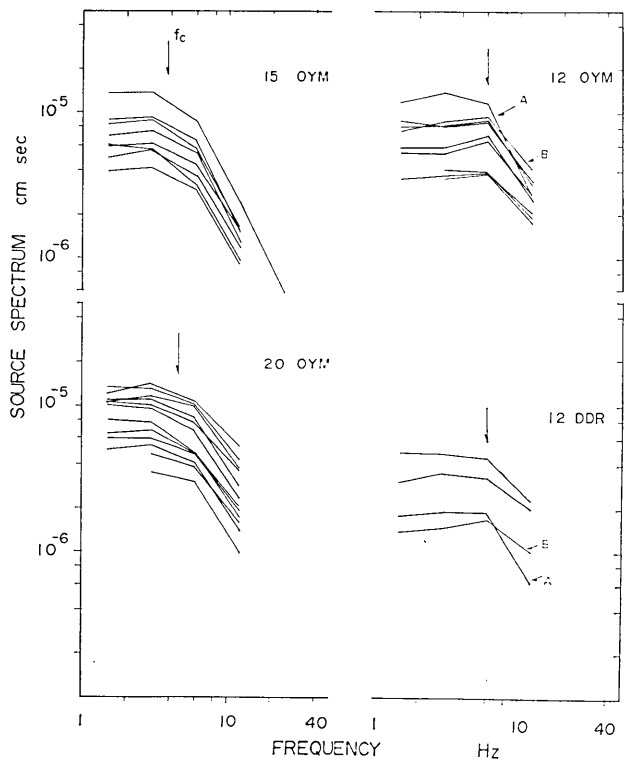

Fig. 14. An example of the source spectra of *SH* waves observed at OYM and DDR.

tion of attenuation. A Q_β 500 is somewhat larger compared with our previous study (TSUJIURA, 1978b), because DDR has a small array station, and the data used in this study is made by the No. 5 station which is the best station of the array (TSUJIURA, 1978a). The spectra of two events recorded commonly with adequate amplitudes at two stations are examined in order to see the adequacy of the choice of Q values. They show nearly the same corner frequency as indicated by the spectra of A and B. The level of flat low frequencies and the corner frequency for larger events therefore can be obtained from the relative values for the common earthquakes determined at DDR.

From each flat low frequencies level (Ω_0), we determine the corresponding seismic moment (M_0) by using Brune's model (BRUNE, 1970), namely

$$M_0 = \frac{1}{c} 4\pi\rho\beta^3 R\Omega_0$$

where R is the hypocentral distance, ρ is the density, β is the shear-wave velocity and c is a geometrical factor. The seismic moment corresponding to each low frequency level was estimated assuming $\beta=3.5$ km/sec, $\rho=2.8$ g/cm^3 and $c=0.8$ (THATCHER and HANKS, 1973). The results show the seismic moments of, on the average, 1×10^{19} dyne cm for $M=1.5$ and 3.5×10^{20} dyne cm for $M=3$ earthquakes, respectively.

Using the circular crack model of MADARIAGA (1976) who gives the relation of $f_c=0.21\ \beta/a$, we estimated the fault radius (a) corresponding to the corner frequency (f_c), assuming $\beta=3.5$ km/sec and found a range of 120 to 200 meters depending on the event group. The source radii in a given event group are nearly constant in spite of a difference in moment by more than a factor of 10.

Using the moment and source radius obtained above, a value of slip length is determined by the following equation

$$M_0 = \frac{2\pi}{3} \mu \Delta U a^2 \qquad \text{(BRUNE, 1970)}$$

where M_0 is seismic moment, μ is rigidity, ΔU is the slip and a is the radius of the crack obtained from the corner frequency. We found the values of the slip of 3.5 cm for $M=3$ and 0.1 cm for $M=1.5$ earthquakes, assuming $\mu=3\times10^{11}$ dyne cm^2. As described in the preceding section, the swarm sequence consists of many event groups. If we assume that the earthquakes in a given event group occur on the same fault as a repeated sliding of the fault, the cumulative slipping length for each group can be estimated by the summation of slip length for each event within the group. Their results are shown in Table 1 together with the event parameter. A comparison of these values to

Table 1. List of earthquake groups with their own spectral features. N: number of earthquakes, f_c: corner frequency, a: source radius determined from corner frequency, $\Sigma \Delta U$: cumulative slipping length.

No.	Date	Time h m h m	N	f_c Hz	a m	$\Sigma \Delta U$ cm
1	Nov. 29 Dec. 3 Dec. 4	2325-2358 1855-1941 0742-0800	20	6	122	9.3
2	Nov. 29 Nov. 30	2308-2350 1123-1124	5	6	122	1.5
3	Dec. 1 Dec. 1 Dec. 1	0619-0650 0907-0923 1252-1500	17	6	122	3.7
3*	Dec. 3	0323-0337	5	4.8	153	1.3
4	Dec. 1 Dec. 1	0719-0835 1239-1240	14	6	122	6.1
5	Dec. 1 Dec. 1 Dec. 2	1024-1151 1617-1618 0033-0036	10	6	122	10.7
6	Dec. 1 Dec. 1 Dec. 2	1115-1241 2008-2036 0017-0031	25	6	122	7.4
7	Dec. 2	0047-0053	6	5	148	7.0
8	Dec. 2 Dec. 2	0105-0106 0308-0414	6	6	122	2.4
9	Dec. 2 Dec. 3	2000-2047 0325-0340	26	6	122	9.0
9*	Dec. 2 Dec. 3	2013-2113 0344-0356	18	4.5	163	4.4
12	Dec. 3 Dec. 4	1818-1836 0707-0708	13	6	122	7.0
13	Dec. 3	1822-1844	11	6	122	11.1
15	Dec. 4 Dec. 5	0813-0905 0036-0037	8	3.8	193	1.7
16	Dec. 4 Dec. 4 Dec. 5	1624-1722 2209-2210 0048-0141	6	6	122	3.1
17	Dec. 5	0029-0105	5	4.5	163	1.2
18	Dec. 6	0614-0619	7	6	122	1.4
19	Dec. 7	1526-1542	14	5	148	5.0
20	Dec. 7 Dec. 7	1546-1555 1557-1729	6 26	5 4.8	148 153	2.8 11.5
22	Dec. 7	1611-1707	8	4.5	163	4.9
23	Dec. 8	0759-0855	8	5	148	2.0

the other evidence, such as the data of crustal movement and gravity change will be useful. The largest earthquake of M5.4 (JMA) which was excluded in this study, however, contributes most of seismic moment and slip. The moment and slip of this earthquake, estimated using the data of wide-band seismograph at DDR, shows a value of $M_0 = 3 \times 10^{23}$ dyne cm and $\Delta U = 50$ cm, respectively.

Discussion

From the analysis of the waveform and the spectrum, we found the salient features of the earthquake swarm activity. They are: Earthquakes with similar waveforms are generated by a source with a linear dimension of about 200-400 meters. They are separated by at most only 100 meters. There are two possible ideas to explain the above conclusion. Either, one, the earthquakes in a given event group occurred independently within an area of about 100 meters, or, two, they occurred on the same fault, such as the repeated sliding of a fault, called "stick slip". The 2nd assumption will be more natural for the present result than the first one, because it is rather difficult to understand how so many earthquakes (maximum of 26 earthquakes with magnitudes between 1.5 and 3) with the same source dimension of 200 meters occurred independently within a space of 100 meters. Moreover, OHNAKA (oral communication, 1979) suggests that the waveforms of the stick-slip type in the laboratory experiment show a similar feature. Our observation can be understood also with the aid of a new earthquake model called "barrier model" proposed by DAS and AKI (1977). The existence of the 19 event groups with their own spectral signature within an area of about 5×8 km will be the result reflecting the existence of numerous cracks and faults bounded by barriers with high strength.

Conclusion

The earthquake swarm activity in the Kawanazaki-oki area of the Izu peninsula was studied using 365 earthquakes with magnitudes between 1.5 and 3. Their spectral features differ significantly from the normal seismic activity. The earthquakes generated within 1 hour consisted mainly of those with similar waveforms. Also, the relative travel times for some isolated waves, such as P and S waves, are common within an error range of 0.05 sec. Especially when the earthquakes with similar size are compared, frequently their waveforms coincide completely from P-wave onset till coda waves. Similar behavior, but with different waveforms are seen for the earthquake group generated at other times of the swarm activity. The 19 event groups

each containing at least five events with similar waveforms are identified for 264 earthquakes selected from the 365 earthquakes.

Considering the waveforms and the time dependence of several isolated waves, it is expected that the earthquakes belonging to each group are distributed within a space of about 100 meters. The 19 event groups with their own spectral features then suggest the migration of the area of swarm activity. In addition, the source spectra obtained at each event group show identical forms with similar corner frequency for the magnitude range between 1.5 and 3. From the view point of waveforms and spectra, we may suggest that there exist numerous cracks and faults enclosed by strong barriers, and the earthquakes in a given event group are occurring on the same fault as a series of stick-slip or repeated incomplete ruptures. If such features are always observed for swarm activities, the present finding will be useful for the discrimination of swarm activity from the other seismic activity such as foreshocks of a major earthquake.

Acknowledgment

The writer wishes to express his thanks to Prof. Keiiti Aki who read the manuscript critically and offered many valuable suggestions. The writer also thanks to Dr. Kenshiro Tsumura and the staff of the expedition team of the earthquake swarm for the use of the data of epicenters.

References

AKI, K. and B. CHOUET, 1975, Origin of coda waves: source, attenuation, and scattering effect, *J. Geophys. Res.*, **80**, 3322-3342.

BRUNE, J. N., 1970, Tectonic stress and the spectra of seismic shear waves from earthquakes, *J. Geophys. Res.*, **75**, 4997-5009.

DAS, S. and K. AKI, 1977, Fault plane with barriers: a versatile earthquake model, *J. Geophys. Res.*, **82**, 5658-5670.

HAMAGUCHI, H. and A. HASEGAWA, 1975, Recurrent occurrence of the earthquake with similar wave forms and its related problems, *Zisin*, **28**, No. 2, 153-169, (in Japanese).

HORI, M., 1973, Determination of earthquake magnitude of the local and near earthquake by the Dodaira Micro-earthquake Observatory, *Speci. Bull. Earthq. Res. Inst.*, **10** (4), 1-4, (in Japanese).

KASAHARA, K. and R. TEISSEYRE, 1966, A dislocation model of earthquake swarms, *Bull. Earthq. Res. Inst.*, **44**, 793-810.

KISHINOUYE, F., 1937, Frequency-distribution of the Itô earthquake swarm of 1930, *Bull. Earthq. Res. Inst.*, **15**, 785-827.

MADARIAGA, R., 1976, The dynamics of an expanding circular fault, *Bull. Seism. Soc. Am.*, **66**, 639-666.

MOGI, K., 1963, Some discussion on aftershocks, foreshocks and earthquake swarms—the fracture of a semi-infinite body caused by an inner stress origin and its relation to the earthquake phenomena (third paper), *Bull. Earthq. Res. Inst.*, **41**, 615-658.

STAUDER, W. and A. RYALL, 1967, Spatial distribution and source mechanism of micro-earthquakes in central Nevada, *Bull. Seis. Soc. Am.*, **57**, 1317-1345.

THATCHER, W. and T.C. HANKS, 1973, Source parameters of southern California earthquakes, *J. Geophys. Res.*, **78**, 8547-8576.

TSUJIURA, M., 1966, Frequency analysis of seismic waves (1), *Bull. Earthq. Res. Inst.*, **44**, 873-891.

TSUJIURA, M., 1973, Spectrum of seismic waves and its dependence on magnitude (1), *J. Phys. Earth*, **21**, 373-391.

TSUJIURA, M., 1977, Spectral features of foreshocks, *Bull. Earthq. Res. Inst.*, **52**, 357-371.

TSUJIURA, M., 1978a, Spectral analysis of the coda waves from local earthquakes, *Bull. Earthq. Res. Inst.*, **53**, 1-48.

TSUJIURA, M., 1978b, Spectral analysis of seismic waves for a sequence of foreshocks, main shock and aftershocks: the Izu-Oshima-kinkai earthquake of 1978, *Bull. Earthq. Res. Inst.*, **53**, 741-759, (in Japanese).

TSUJIURA, M., 1979, The difference between foreshocks and earthquake swarms, as inferred from the similarity of seismic waveform (Preliminary report), *Bull. Earthq. Res. Inst.*, **54**, 309-315, (in Japanese).

TSUMURA, K., I. KARAKAMA, I. OGINO, M. TAKAHASHI, I. NAKAMURA and K. KANJO, 1979, Earthquake swarm off Kawanazaki, Izu Peninsula, *Abstract for Ann. Meet. Seismol. Soc. Japan*, 1, (in Japanese).

---

19. 波形解析からみた伊豆半島川奈崎沖群発地震の活動様式

地震研究所 辻 浦 賢

1978 年 11 月 24 日頃より，伊豆半島，川奈崎沖において地震活動が活発化し約 20 日間続いた．この地震は，その活動状況からみて典型的な群発地震であった．今回これらの地震について，地震波動の波形並びにスペクトル解析から，その活動様式についていくつかの特徴ある結果を得た．主な結果は次の通りである．

（1） 大山観測所上下動成分の早送り記録 (25 mm/sec) の重ね合せにより波形について調べた結果，ある限られた時間帯 (例えば，1 時間) に発生する群発地震の波形は非常に似ており，いわゆる“相似地震”によって構成されていることが解った．更にこのような傾向は，互いに方向の異なる他の観測所の記録についても同じである．

（2） 一連の相似地震には S 波を含むいくつかの孤立波形が見られる．初動から測ったそれぞれの孤立波形の到達時刻は 0.05 sec の範囲内で一致し，特に同じ大きさを持つ地震についてみると，初動から 20 sec 後の Coda wave についても同様の傾向が見られる．

（3） S 波についてのスペクトル解析から，相似地震の Corner frequency は $M=1.5-3$ の間で略一定である．

合計 365 個 ($M \geqq 1.5$) の観測された地震のうち，相似波形を持つ地震数 5 個以上のものを 1 組の相似地震群とすると，全体として約 72% のものが，いずれかの組に属する相似地震であり，計 19 種類の相似地震群が得られた．(1), (2), (3) の結果からみて，それぞれの相似地震は，ある限られたせまい範囲，例えば同じ断層面上で繰返し発生していることが推定され，又 19 種類の相似地震の存在は群発地震の活動域が順次移動していったことを示すものであろう．